4-27-2022

KOH vs Deionized Water Operation in Anion Exchange Membrane Electrolyzers

Noor Ul Hassan

Yiwei Zheng

Paul A. Kohl

Mustain E. William
University of South Carolina, mustainw@mailbox.sc.edu

Publication Info

Published in *Journal of the The Electrochemical Society*, Volume 169, 2022, pages 044526-.

KOH vs Deionized Water Operation in Anion Exchange Membrane Electrolyzers

Journal of The Electrochemical Society, 2022 **169** 044526

KOH vs Deionized Water Operation in Anion Exchange Membrane Electrolyzers

Noor Ul Hassan,[1,*] Yiwei Zheng,[1,*] Paul A. Kohl,[2,] and William E. Mustain[1,*,z]**

[1]*Department of Chemical Engineering, University of South Carolina, Columbia, South Carolina 29208, United States of America*
[2]*School of Chemical and Biomolecular Engineering, Georgia Institute of Technology, Atlanta, Georgia 30318, United States of America*

Anion exchange membrane water electrolyzers (AEMELs) have recently received significant attention due to their potential advantages over proton exchange membrane electrolyzers (PEMELs). However, some AEMELs feed an aqueous salt solution to the cell where PEMELs typically feed deionized (DI) water. DI water is preferred to keep the system and maintenance costs low. Because of this, many AEMEL researchers report performance both in the salt solution (typically KOH) and DI water. However, the methodology for switching between KOH and DI water is often poorly defined, and it is unclear what impact the residual salt has on cell performance after switching from salt to DI water. Having a fully deionized environment is important because the presence of salts in the water feed increase the effective electrochemical surface area of the catalyst in the three-dimensional electrode and residual salt remaining after switching to DI water feed can have a misleading transient effect on cell performance. This paper focuses on understanding the transition from KOH to DI water testing in AEMELs. It is shown that when switching from salt to DI water feed, a large volume of DI water must be fed over several hours to achieve true DI-water performance. It is also shown that starting AEMELs from the beginning with DI water feed (without any KOH ever being fed to the cell) results in better cell durability. Lastly, a cell is demonstrated having operated exclusively on DI water at 1.0 A cm^{-2} for 500 h at an operating voltage of ca. 2 V and a low degradation rate.

 [DOI: 10.1149/1945-7111/ac5f1d]

Manuscript submitted January 6, 2022; revised manuscript received February 15, 2022. Published April 27, 2022. *This paper is part of the JES Focus Issue on Advanced Electrolysis for Renewable Energy Storage.*

Supplementary material for this article is available online

Significant progress has been made in reducing the cost of energy systems that rely on renewable sources such as wind, tidal and solar.[1] However, the intermittent nature of each of these does not allow them to temporally balance their energy supply with the grid demand.[2–6] Electrical energy produced from these systems can be converted to chemical energy carriers such as hydrogen, especially during non-peak hours. By directly utilizing low-cost, off-peak electrical energy, the cost of hydrogen via electrolysis could be lower than conventional processes including steam reforming.[7] The resulting hydrogen can then be utilized for chemical reactions or used to generate power from an internal combustion engine or fuel cell. Hydrogen can also be stored or transported over long distances.

Water electrolysis is a well-established technique for converting water into molecular hydrogen and oxygen at relatively low temperatures. Among low-temperature electrolysis systems (< 100 °C), the alkaline water electrolyzer (AWE) using a liquid electrolyte is the most well-established technology, having already been commercialized for decades with low-cost catalysts and cell components.[8,9] However, they do have three important limitations.[10,11] The first limitation is that the AWE operates at low current density, which leads to large systems with relatively expensive balance of plant.[9,12] The second limitation is that they are fed a concentrated alkaline (aqueous KOH) solution as the electrolyte, which provides both the water for electrolysis and cell-level ionic conductivity. The concentrated KOH is a plant-level safety hazard and it also leads to relatively high maintenance costs.[12] Finally, the AWE can only discharge low pressure hydrogen, which must be mechanically compressed, due to the fluidic nature of the liquid electrolyte.[13–16] To overcome these issues, the proton exchange membrane electrolyzer (PEMEL) was developed. A PEMEL can operate at higher current density than an AWE, giving it a more compact design.[14,17,18] The solid polymer electrolyte in a PEMEL also enables the discharge of pressurized hydrogen (so-called electrochemical compression). However, the cost of PEMEL systems is still relatively high due to the use platinum group metal catalysts and perfluorinated membranes-561.[19,20] Therefore, there is an incentive to combine the high pH advantages of an AWE (i.e., low cost catalysts and membranes) with the solid-state advantages of a PEMEL to create the anion-exchange-membrane electrolyzer (AEMEL).[18,21,22] The goal is to achieve high current density, low gas cross-over, pressurized discharge gas without the high-cost PEMEL components.

Over the past several years, AEMEL performance has significantly improved. Many of the reported cells operate with an aqueous salt feed solution (either KOH or carbonate), although typically at a lower concentration than in an AWE. Regarding performance, Wang et al.[23] reported a current density of 400 mA cm^{-2} at 1.8 V and 50 °C using Pt black as the hydrogen evolution reaction (HER) cathode electrocatalyst and IrOx as the oxygen evolution reaction (OER) anode electrocatalyst. However, the durability was poor in pure DI water. Li et al.,[24] utilized a high IEC ionomer (3.3 meq g^{-1}) to achieve an operating current of 906 mA cm^{-2} at 1.8 V. However, due to high water uptake and solubility of their high IEC ionomer the catalyst was washed away, resulting in somewhat high degradation rates in short term testing, and poor durability in long term testing. Most recently, Yan and coworkers[25] reported 1020 mA cm^{-2} at 1.8 V in pure water. However, the degradation rate was high at both low current density (0.56 mV h^{-1} at 200 mA cm^{-2}) and high current density (1.81 mV h^{-1} at 500 mA cm^{-2}). In fact, the degradation rates for AEMELs are presently much higher than PEMELs, ranging from 0.1 − 2 mV h^{-1}[24] while PEMELs have degradation rates that typically range from 2–10 μV h^{-1}.[26] Therefore, the AEMEL remains a relatively new technology and a significant improvement is needed to achieve high performance and durability.

One of the main AEMEL challenges to achieving low-cost performance is the development of highly active PGM-free catalysts for both the OER and HER. Hiao and Lu et al.,[27] used PGM-free catalysts (Ni−Mo in the cathode and Ni−Fe in the anode) and a self-made membrane and ionomer to achieve a current density of

*Electrochemical Society Member.
**Electrochemical Society Fellow.
[z]E-mail: mustainw@mailbox.sc.edu

300 mA cm^{-2} at 1.8 V. However, the cell was able to operate effectively for only 8 h. An additional issue with AEMELs is the need for durable, low-cost cell components including porous transport layers (PTL) to make the three-dimensional electrodes. It was recently shown that the PTL with a small fiber size and smooth surface results in enhanced performance likely due to its large contact area, higher catalyst utilization, and decreased lateral catalyst-layer electrical resistance.[28,29] Similar studies have also been reported on graded-pore structures to improve mass transport during in PEMWEs.[30,31]

Lastly, to simplify the balance-of-plant, and reduce maintenance, it is preferable to operate membrane-based electrolyzers with deionized water (DI) feed. As discussed above, this is already done in PEMELs; however, most of the reported AEMELs in the literature use carbonate or hydroxide-based electrolytes. The electrolyte feed is used to increase the electrochemically active surface area of the anode electrode where the OER occurs.[32] Moreover, the adsorption of metal cations like K^+ can stabilize the transition state of the water dissociation step promoting HER.[33] K^+ may also enhance the OER by enabling a lattice oxygen-mediated mechanism.[34] When DI water is fed to the cell, typically the performance is lower, with the operating voltage at 1.0 A cm^{-2} increasing by 300 mV or more (Supplementary Table SI (available online at stacks.iop.org/JES/169/044526/mmedia)). Some recent studies have reported good AEMEL performance with DI water, achieving 1.0 A cm^{-2} below 2.0 V.[24,25,35] However, DI water feed tests are typically performed by first breaking-in (break-in is used here to describe a startup procedure meant to activate an MEA for stable operation before collecting polarization scans and steady-state performance evaluation) the cell with an aqueous KOH feed, then replacing the KOH feed in favor of a DI water feed.[25,35,36] As shown in Supplementary Table SII, different protocols are used to transition from KOH to DI water feed in terms of the amount of DI water fed to the cell as well as the time that the cell is exposed to DI water before performing the electrolysis tests. There are also many studies where the protocol to transition from KOH to DI water operation is either poorly described or not described at all. Because residual alkaline electrolyte in the cell can enhance transient activity, it has been previously noted by Lindquist et al. that it is very important that all excess salt from feeding KOH is flushed from the cell before claiming DI water operation.[37] Because of the uncertainty in the procedures to transition from KOH to DI water feed in the literature, as well as some that have very short flushing times, it is possible that some of the reported operating voltages may not be accurate representations of true DI water performance.

Therefore, the primary purpose of this communication is to probe the transition of AEMELs initially operated with KOH to true DI water operation. This was done through a combination of experiments. First, cells were operated at steady-state for several hours with aqueous KOH fed to the anode only. Then, the feed was shifted from KOH to DI water and the voltage response was observed over a 100 h period. During the transition, polarization curves were collected and electrochemical impedance spectroscopy (EIS) was performed. In addition, exposure to any amount of KOH might lead to chemical or mechanical changes in the cell from degradation due to the high anode operating potential. Thus, cells were also broken-in on DI water without any aqueous KOH exposure and their performance and durability are discussed.

Materials and Methods

Catalyst and polymer materials.—A platinum-nickel (PtNi, Pajarito Powder) catalyst was used at the cathode electrode for the HER. The catalyst was deposited onto a Toray-60 carbon paper porous transport layer (PTL) with 5% wetproofing (Fuel Cell Store). At the anode, iridium oxide (IrOx, Nel Hydrogen) was used as the OER catalyst and a nickel fiber felt (300 μm, Dioxide Materials) was used as the PTL. The AEM was a 30 μm-thick functionalized and quaternized poly(norbornene) polymer film, sold as XION™ Composite-72–10CL-30 μm (72% halogenated monomer and 10 mol % crosslinker) by Xergy, Inc. The anode and cathode ionomers were also poly(norbornene)-based. At the anode, an ionomer with 32% halogenated monomer (GT32; IEC = 1.88) was used and at the cathode an ionomer with 69% halogenated monomer (GT69; IEC = 3.46) was used. GT32 and GT69 were synthesized and characterized as reported previously.[38–43]

Electrode fabrication.—The anode (OER) and cathode (HER) electrodes were prepared by hand spraying a catalyst ink directly onto the PTLs. The ink preparation method was adapted from our previous work.[42,43] The formulation of the anode and cathode were different as detailed below. At the anode, a typical process began by soaking 50 mg of GT32 in DI water (1–2 ml) for 30 min. Then, the swollen ionomer was ground with a mortar and pestle for 10 min to allow it to break up into fine particles. Next, 250 mg of the catalyst was added to the mortar along with 20 mg of PTFE powder (Ultraflon MP-25, Fuel Cell Store—added to help with water transport as the bubbles are released from the catalyst layer[42,43]), and the materials were further ground for 10 min, forming a uniform paste. Then, 9–10 ml of 2-propanol (IPA) were added to convert the slurry into a uniformly dispersed ink. The ink was then transferred into a vial and sonicated in an ice bath for 60 min. Simultaneously, a 10% ionomer (25 mg) solution in IPA was prepared and sonicated (ionomer/IPA solution). Half of the ionomer/IPA solution was sprayed onto a 25 cm^2 PTL as a base layer using an Iwata spray gun. Then, the catalyst layer was sprayed onto the base layer using an identical spray gun. Next, the other half of the ionomer/IPA solution was sprayed on top of the catalyst layer as a final coating layer. Finally, the catalyst-coated PTLs were cut into smaller electrodes for testing.

An identical procedure was applied for preparing the cathode ink. The catalyst:ionomer weight ratio in cathode was 4:1 while it was 3:1 in the anode. Typically, 30 mg of GT69 ionomer and 200 mg of catalyst were used. In addition, 16 mg of PTFE powder (Ultraflon MP-25, Fuel Cell Store) was added to increase the hydrophobicity of the electrode. Toray TGP-H-060 with 5% wetproofing was used for the cathode PTLs.

AEM electrolyzer assembly and testing.—The AEMs and electrodes were ion exchanged in a 1.0 M KOH solution for a total of 60 min (refreshing the solution every 20 min) prior to cell assembly. Excess surface KOH was removed from the electrodes and AEM by rinsing with DI water, followed by lightly dabbing with Kimwipes prior to MEA assembly. The poly(norbornene) AEM was sandwiched between the two electrodes and pressed together in the hardware with no prior hot pressing. The custom cell hardware had an active area of 5.0 cm^2. The anode flowfield was made from 316 stainless steel while the cathode flow field was made from graphite. The anode and cathode flowfields both had single serpentine channels. Appropriate thickness gaskets were used to provide suitable MEA compression, with a target of 25%. The torque applied to the cell hardware was 40 in-lb. Once assembled, the lab-scale AEMELs were tested using a custom-built electrolysis test station powered by an Arbin Model BT-2000. All tests were performed at a cell temperature of 60 °C. All cells were fed either 0.3 M KOH solution in 18.2 MΩ·cm DI water or pure DI water to the anode side only at a rate of $\sim$ 2 ml min^{-1} using a BT100S Basic Variable Speed Peristaltic Pump with Pump Head YT25. The feed solution was preheated to 60 °C before being fed to the electrolyzer cell. The cathode inlet was closed while the outlet was fed to a bubbler to visualize hydrogen evolution before being sent to the building exhaust. The cathode effluent was periodically fed to a Thermo Fisher Scientific GFM Pro Flowmeter in order to measure the volumetric flowrate of the evolved gas. This was then used to determine the faradaic efficiency of the operating cells.

To begin cell testing, each cell was equilibrated to the desired temperature for 30 to 60 min at zero current with the desired feed solution. The cell was conditioned by applying a small current (100

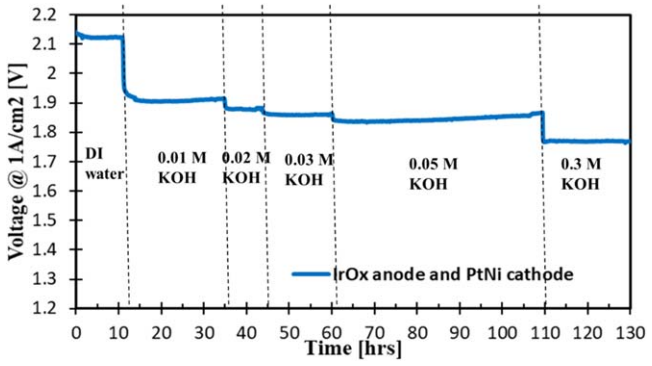

Figure 1. Operation of an AEMEL at 1.0 A cm^{-2} and 60 °C with various concentrations of added KOH. The cells were first operated with DI water and no initial KOH feed. Anode: IrOx catalyst with GT69 ionomer. Cathode: PtNi catalyst with GT-32 ionomer; AEM: GT72–10 (30 μm).

mA cm^{-2}) and waiting for the voltage to equilibrate, which typically took 30 to 60 min. After the cells equilibrated, polarization curves were collected from 1.3 V to 2.4 V at 20 mV s^{-1} scan rate. Then, steady state voltage measurements were collected at a constant current density of 1.0 A cm^{-2}.

Electrochemical impedance spectroscopy.—Electrochemical impedance spectroscopy (EIS) was also used to investigate the behavior of the cells. EIS is a very common experimental technique where a small alternating current (AC) current or voltage signal is imposed on an electrochemical device and the amplitude and phase shift of the response are monitored. EIS experiments were carried out from 0.1 Hz to 10 kHz with an amplitude of 5% of the applied current. The resulting data was fit to an appropriate equivalent circuit model and important properties of the cell including Ohmic resistance, charge transfer resistance, double layer capacitance and diffusion behavior were extracted. EIS data was collected at three different current densities, 100 mA cm^{-2}, 500 mA cm^{-2} and 1000 mA cm^{-2} while cell operated on 0.3 M KOH and DI water feed.

Results and Discussion

Transition from KOH to DI water operation.—As mentioned earlier, different protocols are used in the AEMEL research community for cell break-in before operating while being fed DI water. This can lead to uncertainty with regards to the accuracy of reported data while flowing DI water due to the presence of residual base. Polarization curves are typically collected while the cell is operated with solutions of various concentrations of alkaline solution, starting from salt solutions and ending in DI water. One of the main issues with this approach is that any residual KOH in the operating cell could erroneously boost the cell performance, showing high performance with DI water. Therefore, this work started from the opposite direction, where the cell was initially broken in at steady state with a DI water feed. Then, increasing concentrations of KOH were fed to the cell. The results are shown in Fig. 1 for an AEMEL operating at 1.0 A cm^{-2} and 60 °C. For the first 12 h, the cell was fed 18.2 MΩ DI water. Under this condition, the cell started at a voltage of 2.15 V, settling down to a steady-state value of 2.11 V. After this initial operation on DI water, the feed was replaced with 0.01 M KOH solution and the operating voltage dropped precipitously to just over 1.9 V. This >200 mV drop in the cell operating voltage with very dilute KOH shows how trace amounts of KOH in the cells can affect the operating voltage. Next, the electrolyte was progressively changed to feed solutions with higher KOH concentration. Every increase in KOH concentration improved the cell operating voltage. The final electrolyte fed to the cell was 0.3 M KOH, which had a stable operating voltage of ~1.75 V, which is 350 mV lower than true DI water operation.

The results in Fig. 1 call into question any studies in the literature where polarization curves were collected relatively quickly after being operated initially with an alkaline solution (0.1–1 M KOH) and then switched to DI water. It is our contention that many of those cells did not purge the cell for a long enough time with a sufficient volume of DI water. Hence, they still contain significant KOH in the cell. This statement is supported by Lindquist et al.,[37] who showed that there is a significant difference in the performance of cells based on the amount of time that they were flushed with DI water after KOH operation. To show the role of trapped KOH on cell behavior, we started a cell operating on 0.3 M KOH. The polarization curve for the aqueous 0.3 M KOH feed is shown as red triangles in Fig. 2a. At this condition, a cell voltage of 1.71 V was recorded at a current density of 1.0 A cm^{-2}. This voltage response is comparable to literature reports utilizing noble metal-based catalysts and similar operating conditions.

Next, the cell feed was switched to DI water. To initiate this, DI water was fed to the cell at open circuit at flowrate of ~ 50 ml min^{-1} for 5 min. Then, the DI water flowrate was reduced to the typical value of 2 ml min^{-1}. A polarization curve (Green diamonds) was collected at this point and the polarization curve nearly overlaps with the polarization curve taken with 0.3 M KOH. There was only a small deviation at higher currents where the operating voltage was increased to 1.74 V at 1.0 A cm^{-2}. Continuing with the same water flowrate, after 1 h (where ~350 ml of DI water had been fed), another polarization curve was collected, shown as orange squares in Fig. 2a. This polarization curve showed similar behavior in the kinetic region to the first two polarization curves, but there was a clear increase in the Ohmic resistance of the cell. At 1.0 A cm^{-2}, a voltage of 1.8 V was recorded, which is slightly higher than operation with 0.3 M KOH. However, a clearer picture of what is happening is shown in transient response experiment in Fig. 2b where a cell was operated at a constant current density of 1.0 A cm^{-2} for 100 h. For the first ca. 5 h, the cell was operated on 0.3 M

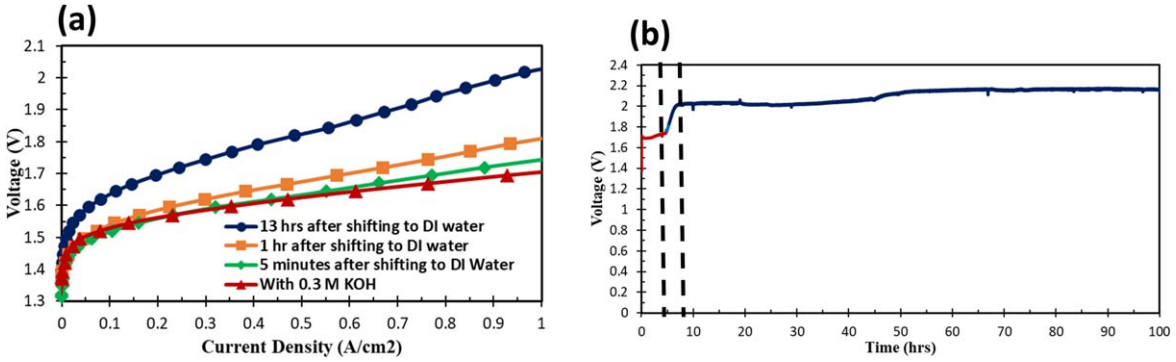

Figure 2. (a). Polarization curves collected at start of the cell operation on 0.3 M KOH and then at different times while the cell was switched to DI water feed. (b). Steady state voltage response of the cell initially operated with 0.3 M KOH and then switched to DI water while operating at a constant current density of 1.0 A cm^{-2}. AEM: GT-72–10 (30 μm), IrOx as OER electrocatalyst and PtNi as HER electrocatalyst. Cell operated with no backpressure at cell temperature 60 °C.

KOH, where a steady-state voltage nearly identical to the polarization curve was observed. Then, the cell was switched to DI water. From that point, the voltage rose and it took the cell more than 3 h to reach the new steady state voltage of just over 2.0 V, a 300 mV increase. After only 1 h on DI water feed, the cell voltage was just over 1.8 V. Based on this, it is clear that after 1 h of DI water feed (even in Fig. 2a where 350 ml of water had been run through the cell), there is still residual KOH in the cell that is affecting the cell performance. To show the importance of adequately flushing the cell before taking DI water fed polarization curves, a polarization curve was taken after 13 h of constant DI water flow and the resulting polarization curve (indicating true DI water operation) is shown as blue diamonds in Fig. 2a. The polarization curve collected after 13 h (Fig. 2a) shows a clear loss in performance. It also shows an operating voltage at 1.0 A cm^{-2} that exactly corresponds to the steady state value in Fig. 2b, suggesting that the true voltage response on DI water had been achieved. It is noteworthy that the total volume of DI water flowed through the cell during this time was ~2 L, which is larger than typical in the literature for switching from KOH to DI water feed. Based on Figs. 2a and 2b, it appears that an appropriate standard procedure would be to flush all AEMELs for at least 5 h before taking a polarization curve meant to represent pure DI water conditions, and longer times are even better.

Lastly, once the cell reached true DI water operation, it was allowed to run at steady state until 100 total hr was achieved (Fig. 2b). During this time, the cell voltage increased to ~ 2.15 V at a degradation rate of around 1.3 mV h^{-1}. It is possible that this increased operating voltage is related to membrane, ionomer, or catalyst degradation initiated by the harsh initial alkaline environment in the AEMEL anode at the beginning of testing—where both high pH and high potential are present. All of those components perform efficiently on alkaline feed, however, that feed can have a detrimental effect on long term durability.

To show the possible effects of the electrolyte concentration on durability, a cell was broken-in on KOH and set to operate at a constant current density of 1.0 A cm^{-2} for four days. The result is shown in Fig. 3. During polarization, Fig. 3a, the cell voltage at 1.0 A cm^{-2} was again 1.7 V, with low kinetic resistance. At the beginning of the durability test, the operating voltage exactly matched the polarization curve, but over the next 20 h, the voltage increased to 1.8 V (5 mV h^{-1} degradation rate). After 20 h, the cell voltage started to decrease again. Though this may be viewed as a positive sign, it is known that internal short-circuits from physical changes can also lead to this behavior.[24] Such a short would also result in a decrease in the H_2 production rate. Therefore, the hydrogen flowrate was measured at various intervals and it was found that the hydrogen flowrate was reduced by approximately 50% after 50 h operation. This behavior was confirmed by running multiple cells. Therefore, it is likely that although a more concentrated alkaline environment is good for initial performance, it may be detrimental to long-term durability. Even breaking in the cell on alkaline feed and then switching to DI water may be detrimental and could initiate cell degradation, as shown in Fig. 2b.

Electrochemical Impedance Spectroscopy (EIS) measurements.—EIS analysis was performed at three current densities, 100, 500 and 1000 mA cm^{-2}, for cells operated on both 0.3 M KOH and DI water. The resulting Nyquist plots are shown in Fig. 4. Important parameters like Ohmic area-specific resistance (R_s), charge transfer resistance (R_1), and double layer capacitance (Q_1) were extracted. At 100 mA cm^{-2}, the Ohmic resistance of the cell while operating on 0.3 M KOH was 0.21 Ohm cm^2 which increased to 0.26 Ohm cm^2 when operating with DI water feed. At that same current, the charge transfer resistance was 0.44 Ohm cm^2 with 0.3 M KOH and 0.65 Ohm cm^2 with DI water feed. The double layer capacitance was 1.11 F (5 cm^2 area) in 0.3 M KOH which decreased to 0.17 F when cell was switched to DI water feed - indicating a loss in the active surface area. At 500 mA cm^{-2}, the ohmic resistance increased from 0.20 Ohm cm^2 to 0.31 Ohm cm^2 when shifted from alkaline solution to DI water feed while the charge transfer resistance increased from 0.14 Ohm cm^2 to 0.26 Ohm cm^2. At 1000 mA cm^{-2}, the ohmic resistance increased from 0.22 Ohm cm^2 to 0.32 Ohm cm^2 when shifted from alkaline solution to DI water feed while the charge transfer resistance increased from 0.09 Ohm.cm^2 to 0.15 Ohm.cm^2.

Table I shows EIS data parameters obtained by fitting the data with an equivalent circuit at different current densities while operating on 0.3 M KOH and DI water. Both the Ohmic resistance and the charge transfer resistance increased when the operating electrolyte was changed from 0.3 M KOH to DI water feed. The average increase in the Ohmic resistance was 43%. This was driven by a reduction in the charge carrier concentration in when DI water is fed vs KOH. AEMs are well-known to uptake liquid water during operation and DI water is not able to assist with ion transport within the electrode and membrane in the same way as a KOH solution can contribute. KOH feed also offers added benefits of osmotic deswelling, also noted elsewhere.[44] Additionally, the average increase in the charge transfer resistance was 45%. This increase in resistance could be attributed to a reduction in additional ion-transport pathways and ion-transport in the ionomer resulting in a lower electrochemically active surface area (supported by the measured capacitance values) when operating on DI water vs KOH[32] these trends are in agreement with other prior work.[45,46]

Cell break-in and operation on DI water feed.—To investigate if exposure to KOH accelerates AEMEL degradation, it is important to break-in and operate a cell that was never exposed to flowing KOH. That is not to say that DI water operation is completely safe from an AEMEL perspective. Operating an AEMEL on pure water can introduce ionomer swelling, dissolution and poisoning.[10] Cells were assembled with only DI water feed during break-in and operation. Representative data is shown in Fig. 5, with a polarization curve shown in **5a**. For this cell, the operating voltage was around 2 V at 1.0 A cm^{-2}, which is consistent with the data in Fig. 2.

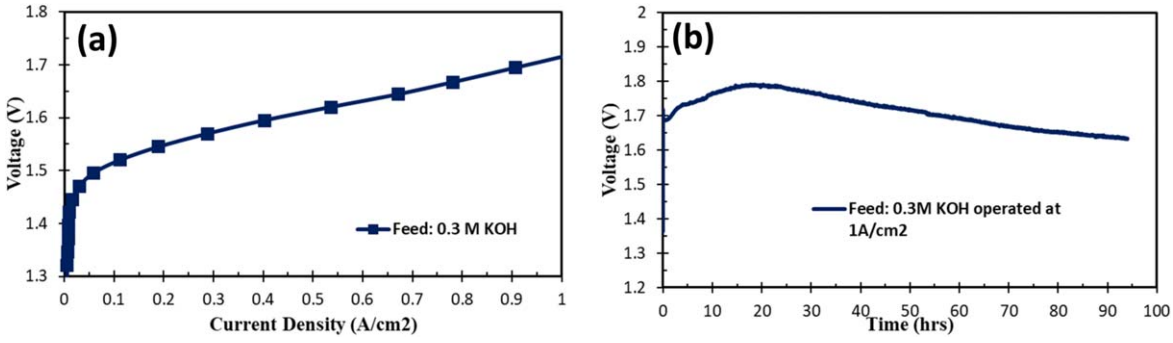

Figure 3. AEMEL (a) polarization curves and (b) durability test (at 1.0 A cm^{-2}) showing the voltage response of a cell that was completely operated while feeding 0.3 M KOH electrolyte. AEM: GT-72–10 (30 μm). Anode catalyst: IrOx. Cathode catalyst: PtNi. Cell temperature: 60 °C.

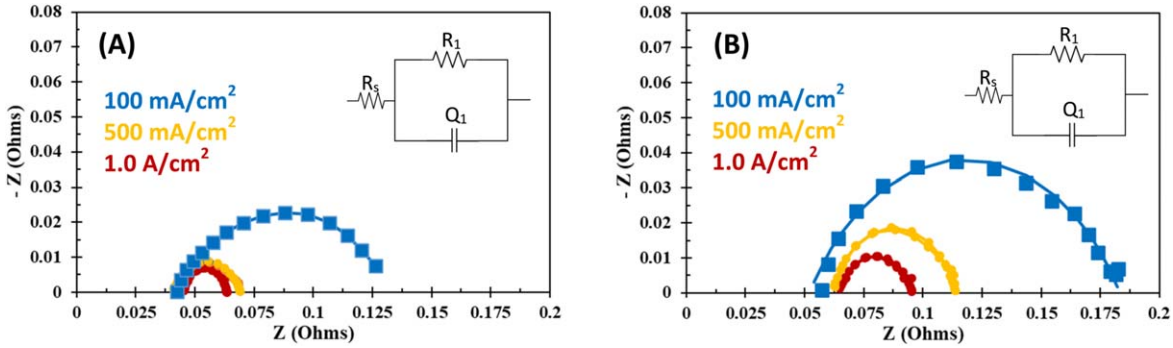

Figure 4. Nyquist plots and circuit analysis for an AEMEL operating at 100 mA cm^{-2} (Blue curves), 500 mA cm^{-2} (Yellow curves) and 1000 mA cm^{-2} (Red curves) operated in (A) 0.3 M KOH; and (B) DI water.

Table I. EIS data parameters obtained by fitting the data with an equivalent circuit at different current densities while operating on (A) 0.3 M KOH and (B) DI water.

	0.3 M KOH			DI water		
Parameter	100 mA cm^{-2}	500 mA cm^{-2}	1000 mA cm^{-2}	100 mA cm^{-2}	500 mA cm^{-2}	1000 mA cm^{-2}
Q_1 (sα/Ω)	1.10661	0.509898	0.178236	0.170222	0.079326	0.153619
α	0.62144	0.708758	0.83654	0.67152	0.790077	0.756816
R_S (Ω)	0.042035	0.040652	0.045338	0.052312	0.0618	0.06441
R_1 (Ω)	0.087624	0.028482	0.018081	0.130921	0.052089	0.031112
X^2	0.011895	0.008204	0.003794	0.030734	0.011121	0.002551

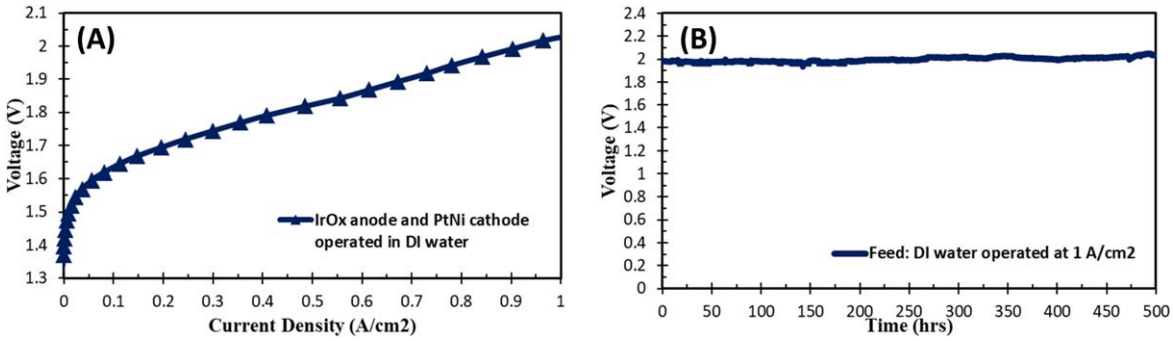

Figure 5. (A) Polarization curves and (B) durability test (at 1.0 A cm^{-2}) for an AEMEL only exposed to DI water during operation. AEM: GT-72–10 (30 μm); Anode: IrOx; Cathode: PtNi. Cell temperature: 60 °C.

Operating at a steady current of 1.0 A cm^{-2}, the cells operated quite stably, with a low degradation rate of 93.5 μV/h over 500 h. It should also be noted that the DI water pH was monitored during the operational lifetime and was measured to be 7.6 at the end of operation. Lastly, the exiting hydrogen volumetric flowrate was measured during operation, fluctuating at steady state from 39.4 to 40.1 ml min^{-1}, which corresponds to a faradaic efficiency between 98.8%–99.8%, even after 500 h. This data strongly suggests that exposure of AEMELs to KOH at any point during operation can be detrimental to their long-term stability. If the field is to transition to true DI water operation, there is a need to improve the performance, likely by increasing the electrochemical surface area of existing systems without the addition of KOH. Previous reports have investigated the use of carbonates as the supporting electrolyte for these systems, but that leads to other systems-level problems during operation such as carbonate accumulation and lower ion mobility resulting in increased cell resistance. This means that new strategies are needed for cell and component design, including the structure of the catalysts and electrodes as well as their integration into operating AEMELs.

Conclusions

Anion exchange membrane water electrolyzers (AEMELs) promise to lower the cost of hydrogen production. However, there is significant research and development that remains to make these cells and systems commercial-ready. In the AEMEL, the oxygen evolution reaction (OER) electrode dictates much of its performance as it is critical in terms of facilitating water transport to the membrane, removing oxygen bubbles, and enabling anion and electron exchange while flooded in water. This study showed that the performance of the OER electrode is strongly affected by the concentration of supporting electrolyte. Because of this, it is likely that many of the studies in the literature begin their data collection before the AEMEL is fully purged of KOH, which can lead to underprediction of the DI-water operating voltage in these systems. It was also shown that exposure to KOH can be detrimental to cell stability, meaning that there is a balance between performance and durability that needs to be found. A cell operating solely on DI water from its start was able to achieve 500 h life at a low degradation rate, but at a higher operating voltage than desired for commercial applications.

Acknowledgments

The authors gratefully acknowledge the financial support of the U.S. Department of Energy, Office of Energy Efficiency & Renewable Energy H2@Scale program (Award Number: DE-EE0008833).

ORCID

Yiwei Zheng https://orcid.org/0000-0002-6722-5883
Paul A. Kohl https://orcid.org/0000-0001-6267-3647
William E. Mustain https://orcid.org/0000-0001-7804-6410

References

1. Lazard's Levelized Cost of Energy and Levelized Cost of Storage—(2021), (https://lazard.com/perspective/levelized-cost-of-energy-and-levelized-cost-of-storage-2020/#:~:text=Lazard's%20latest%20annual%20Levelized%20 Cost,build%20basis%2C%20continue%20to%20maintain).
2. W. Cole, T. Mai, J. Richards, P. Das, and P. D. Vallett, *National Renewable Energy Lab. (NREL), Usdoe Office of Energy Efficiency and Renewable Energy (EERE* (Golden, CO, USA) (2017).
3. W. Cole, B. Frew, P. Gagnon, A. Reimers, J. Zuboy, and R. Margolis, *Energy*, **155**, 690 (2018).
4. F. Creutzig, P. Agoston, J. Goldschmidt, G. Luderer, G. Nemet, and R. Pietzcker, *Nat. Energy*, **2**, 17140 (2017).
5. D. Heide, L. von Bremen, M. Greiner, C. Hoffmann, M. Speckmann, and S. Bofinger, *Renewable Energy*, **35**, 2483 (2010).
6. J. Apt, *J. Power Sources*, **169**, 369 (2007).
7. B. Pivovar, N. Rustagi, and S. Satyapal, *Electrochem. Soc. Interface*, **27**, 47 (2018).
8. B. Decourt, B. Lajoie, R. Debarre, and O. Soupa, *The Hydrogen-Based Energy Conversion FactBook* (The SBC Energy Institute, Houston, TX, USA) (2014).
9. R. L. LeRoy, *Int. J. Hydrogen Energy*, **8**, 401 (1983).
10. D. Li, A. R. Motz, C. Bae, C. Fujimoto, G. Yang, F. Zhang, K. E. Ayers, and Y. S. Kim, *Energy Environ. Sci.*, **14**, 3393 (2021).
11. R. Abbasi et al., *Adv. Mater.*, **31**, 1805876 (2019).
12. A. Godula-Jopek, *Hydrogen Production by Electrolysis* (Wiley, New York, NY) (2015).
13. M. Bodner, A. Hofer, and V. Hacker, "Wiley interdiscip. Rev." *Energy Environ.*, **4**, 365 (2015).
14. K. E. Ayers, E. B. Anderson, C. Capuano, B. Carter, L. Dalton, G. Hanlon, J. Manco, and M. Niedzwiecki, *ECS Trans.*, **33**, 3 (2010).
15. K. E. Ayers, E. B. Anderson, C. B. Capuano, M. Niedzwiecki, M. A. Hickner, C.-Y. Wang, Y. Leng, and W. Zhao, *ECS Trans.*, **45**, 121 (2013).
16. K. E. Ayers, C. Capuano, and E. B. Anderson, *ECS Trans.*, **41**, 15 (2012).
17. E. Anderson, *Presented at 2nd Int. Workshop on Durability and Degradation Issues in PEM Electrolysis Cells and its Components*, Freiburg, Germany (2016).
18. M. Götz, J. Lefebvre, F. Mörs, A. McDaniel Koch, F. Graf, S. Bajohr, R. Reimert, and T. Kolb, *Renewable Energy*, **85**, 1371 (2016).
19. K. Zeng and D. k. Zhang, *Prog. Energy Combust. Sci.*, **36**, 307 (2010).
20. "EU's Funding programme for research and innovation, Horizon 2020, fuel cells and hydrogen joint undertaking (FCH JU)." *Multi-Annual Work Plan*, 2014https://fch.europa.eu/sites/default/files/FCH%202%20JU%20MAWP-%20final%20%28ID%204221004%29.pdf (2016), accessed on March 2022.
21. A. Lim, M. K. Cho, S. Y. Lee, H.-J. Kim, S. J. Yoo, Y.-E. Sung, J. H. Jang, and H. S. Park, *J. Electrochem. Sci. Technol.*, **8**, 265 (2017).
22. O. Schmidt, A. Gambhir, I. Staffell, A. Hawkes, J. Nelson, and S. Few, *Int. J. Hydrogen Energy*, **42**, 30470 (2017).
23. Y. Leng, G. Chen, A. J. Mendoza, T. B. Tighe, M. A. Hickner, and C. Y. Wang, *J. Am. Chem. Soc.*, **134**, 9054 (2012).
24. D. Li et al., *Nat. Energ.*, **5**, 378 (2020).
25. J. Xiao, A. M. Oliveira, L. Wang, Y. Zhao, T. Wang, J. Wang, B. P. Setzler, and Y. Yan, *ACS Catal.*, **11**, 264 (2021).
26. Q. Feng, X. Z. Yuan, G. Liu, B. Wei, Z. Zhang, H. Li, and H. Wang, *J. Power Sources*, **366**, 33 (2017).
27. L. Xiao, S. Zhang, J. Pan, C. Yang, M. He, L. Zhuang, and J. Lu, *Energy Environ. Sci.*, **5**, 7869 (2012).
28. Q. Xu, S. Z. Oener, G. Lindquist, H. Jiang, C. Li, and S. W. Boettcher, *ACS Energy Lett.*, **6**, 305 (2021).
29. N. U. Hassan, M. Mandal, B. Zulevi, P. A. Kohl, and W. E. Mustain, *Electrochim. Acta*, **409**, 140001 (2021).
30. P. Lettenmeier, S. Kolb, N. Sata, A. Fallisch, L. Zielke, S. Thiele, A. S. Gago, and K. A. Friedrich, *Energy Environ. Sci.*, **10**, 2521 (2017).
31. T. Schuler, J. M. Ciccone, B. Krentscher, F. Marone, C. Peter, T. J. Schmidt, and F. N. Büchi, *Adv. Energy Mater.*, **10**, 1903216 (2020).
32. J. Liu, Z. Kang, D. Li, M. Pak, S. M. Alia, C. Fujimoto, G. Bender, Y. S. Kim, and A. Z. Weber, *J. Electrochem. Soc.*, **168**, 054522 (2021).
33. M. C. O. Monteiro, A. Goyal, P. Moerland, and M. T. M. Koper, *ACS Catal.*, **11**, 14328 (2021).
34. J. A. D. Rosario, G. Li, M. F. M. Labata, J. D. Ocon, and P. A. Chuang, *Appl. Catalysis B*, **288**, 119981 (2021).
35. R. Soni, S. Miyanishi, H. Kuroki, and T. Yamaguchi, *ACS Appl. Energy Mater.*, **4**, 1053 (2020).
36. A. Lim, H. J. Kim, D. Henkensmeier, S. J. Yoo, J. Y. Kim, S. Y. Lee, Y. E. Sung, J. H. Jang, and H. S. Park, *J. Ind. Eng. Chem.*, **76**, 410 (2019).
37. G. A. Lindquist, S. Z. Oener, R. Krivina, A. R. Motz, A. Keane, C. Capuano, K. E. Ayers, and S. W. Boettcher, *ACS Appl. Mater. Interfaces*, **13**, 51917 (2021).
38. M. Mandal, G. Huang, and P. A. Kohl, *J. Membr. Sci.*, **570**, 394 (2019).
39. N. U. Hassan, M. Mandal, G. Huang, H. A. Firouzjaie, P. A. Kohl, and W. E. Mustain, *Adv. Energy Mater.*, **10**, 2001986 (2020).
40. M. Mandal, G. Huang, N. U. Hassan, X. Peng, T. Gu, A. H. Brooks-Starks, B. Bahar, W. E. Mustain, and P. A. Kohl, *J. Electrochem. Soc.*, **167**, 054501 (2020).
41. M. Mandal, G. Huang, N. U. Hassan, W. E. Mustain, and P. A. Kohl, *J. Mater. Chem. A*, **8**, 17568 (2020).
42. G. Huang, M. Mandal, N. H. Hassan, K. Groenhout, A. Dobbs, W. E. Mustain, and P. A. Kohl, *J. Electrochem. Soc.*, **167**, 164514 (2021).
43. G. Huang, M. Mandal, N. H. Hassan, K. Groenhout, A. Dobbs, W. E. Mustain, and P. A. Kohl, *J. Electrochem. Soc.*, **168**, 024503 (2020).
44. I. Vincent, A. Kruger, and D. Bessarabov, *Int. J. of Hydrogen Energy*, **42**, 10752 (2017).
45. A. Baricci, A. Bisello, A. Serov, M. Odgaard, P. Atanssov, and A. Casalegno, *Sustainable Energy & Fuels*, **12**, 3375 (2019).
46. I. Vincent, E. C. Lee, and H. M. Kim, *Sci. Rep.*, **11**, 293 (2021).
47. C. Li and J. B. Baek, *Nano Energy*, **87**, 106162 (2021).